

Age Estimation Based on Complexity-Aware Features

Anonymous ACCV 2014 submission

Paper ID 20

Abstract. The research related to age estimation using face images has become increasingly important. We propose an age estimator using two kinds of local features, the gradient features which well describe the local characteristic, and the Gabor wavelets which reflect the multi-scale directional information. The RealAdaBoost algorithm with a complexity penalty term in the feature selection module is applied to choose meaningful regions from human face for feature extraction, while balancing the discriminative capability and the computation cost at the same time. Furthermore, the hierarchical classifier, which is composed of an age group classification (e.g., 15-39 years old, 40-59 years old etc.) and a detailed age estimation (e.g. 19, 53 years old, etc.) are utilized to get the final age. Experimental results show that the proposed approach outperforms the methods using single feature on PAL and FG-NET database. It also achieves competitive accuracy with the state-of-the-art algorithms.

1 Introduction

Systems based pattern recognition have been proven to be very useful in many areas such as security and access control, human detection, human computer interaction, and brain computer interface. Recently, the research related to age estimation using face images is more important than ever. The potential applications include automatic guest enrollment, parent TV program control, video surveillance, etc.

In general, age estimation systems consist of two steps: feature extraction and classification/regression. The features used in age estimation can be categorized into the local features and the global features. The local features are extracted on some regions which might contain specific facial characteristic, such as wrinkles and freckles. They have been used to classify people into age groups. Conversely, the global features are extracted based on whole face shape or all facial feature points. They are generally used to estimate the exact age. Some researchers also use hybrid features to improve the estimation accuracy, which is the combination of local features and global features.

After feature extraction, the classification/regression module is utilized to train the age estimator. The commonly-used algorithms include the age group classification, single-level estimation and the hierarchical age estimation. Age group classification is an approach that roughly predicts an age group, whereas single-level method focuses on detailed age prediction. The hierarchical method is

045 a coarse-to-fine method which integrates the single-level and age group methods 045
046 together. 046

047 Regarding the efficiency issue, local features based methods perform better 047
048 compared to global features based methods utilizing ASM [1] or AAM [2]. Un- 048
049 fortunately, the use of the local features for age estimation has not been well 049
050 investigated. The methods extracting a dense feature vector for each local re- 050
051 gion in the aligned face might lead to dimension redundant. In addition, using 051
052 dense feature is relatively slow. Some other algorithms use AdaBoost to select 052
053 key dimensions [3] from the dense features. But it is difficult to describe a spe- 053
054 cific pattern using single dimensional feature in complicate recognition tasks. It 054
055 also leads to potential risk of weakening the discriminative power of the resulting 055
056 classifier. 056

057 To solve this problem, we focus on selecting the meaningful regions in hu- 057
058 man face for feature extraction, while dealing with the accuracy and efficiency 058
059 at the same time. This paper has two contributions. Firstly, we integrate three 059
060 kinds of localized features together for age estimation, including SIFT, HOG, 060
061 and Gabor. In addition, different from simply mixing or concatenating these fea- 061
062 tures, we use the complexity-aware RealAdaBoost algorithm, which includes a 062
063 complexity penalty term in the process of feature selection. As a result, both the 063
064 discriminative power and the computation cost of the features are evaluated in 064
065 the training procedure. We divide the training samples into 4 age groups, 0-15, 065
066 16-40, 41-59, and 60+. The above complexity-aware RealAdaBoost is applied to 066
067 select the meaningful regions on each age group respectively. Then the support 067
068 vector machine is utilized to train a hierarchical age estimator based on these 068
069 selected features. Plenty of experiments on public datasets are used to evaluate 069
070 our method. The experimental results show that our approach achieves signifi- 070
071 cant improvement on the estimation accuracy compared to using single features. 071
072 The result is also competitive with the state-of-the-arts approaches in PAL and 072
073 FG-NET database. 073

074 The rest of this paper is organized as follows. Section 2 is the related work. 074
075 Section 3 presents the features used in this paper. Section 4 introduces the 075
076 RealAdaBoost algorithm with the complexity-aware criterion. Section 5 shows 076
077 our experimental results. Conclusion is given in the last section. 077

078 2 RELATED WORK 078

079 079

080 There has been a great number of work about feature extraction for age esti- 080
081 mation. Kwon and Lobo [4] classify facial images into three age groups using 081
082 the distance ratio of facial components and the wrinkles. Hayashi et al. [5] use 082
083 histogram equalization and Hough transform for skin extraction and wrinkle 083
084 detection. A lookup table containing the wrinkle state against appearance at a 084
085 given age and gender is utilized for age estimation. Fukai et al. [6] adopt fast 085
086 Fourier transform to extract features from a face image by genetic algorithms. 086
087 Gao et al. [7] integrate Gabor features and a fuzzy version of Linear Discrimi- 087
088 nant Analysis (LDA) to classify face into various age classes. Mu et al. [8] use 088
089 089

090 biologically inspired features and introduced a new operator to model the aging 090
091 process. Yan et al. [9] combine the local feature and global feature together and 091
092 utilize a hierarchical classifier to improve the performance. 092

093 The problem of age estimation can be converted into a classification/regression 093
094 problem. Classification can be in groups such as babies, teens, adults or 1-5, 5- 094
095 10, 10-15, while the regression method predicts the exact age based on a set of 095
096 coefficients learnt by using suitable loss functions. Lanitis et al. [10] approach the 096
097 problem of age estimation in a regression way. They propose a quadratic function 097
098 where age is dependent on feature vector extracted from the face. Ueki et al. [11] 098
099 introduce a two phased approach based on LDA and 2D-LDA and have used only 099
100 the first four dimensions of the extracted features to make Gaussian classifier 100
101 to classify images in various age groups. Wang et al. [12] propose a novel data 101
102 selection of the Furthest Nearest Neighbour (FNN) that generalizes the margin- 102
103 based uncertainty to the multi-class case to handle large data efficiently in age 103
104 classification. Guo et al. [13] and Liu et al. [14] solve the problem by Support 104
105 Vector Machines (SVM) and Support Vector Regression(SVR). Kohli et al. [15] 105
106 propose a technique which extracts features based on AAM and use a global 106
107 classifier to obtain a rough estimate distinguishing between child/teen-hood and 107
108 adulthood. An improved version of their work based on hierarchical classifier is 108
109 published in [16]. 109
110 110

111 3 FEATURES USED FOR FACE DESCRIPTION 111 112 112

113 In this section, we will introduce the three localized features used in our method, 113
114 SIFT, HOG, and Gabor. 114
115 115

116 3.1 Gradient features 116 117 117

118 Scale Invariant Feature Transform (SIFT) is invariant to scaling, translation and 118
119 rotation, and partially invariant to illumination changes and affine projection. 119
120 Using these descriptors, objects can be reliably recognized even in the case of 120
121 different views, low illumination or occlusion. In SIFT feature extraction, we 121
122 first build a scale space by convolving it with multi-scale Gaussian kernels and 122
123 then calculate the Difference of Gaussian (DoG) between each two adjacent 123
124 scale spaces. The maximum and minimum of the DoG are selected as candidate 124
125 interest points, from which elements with low contrast and edge responses are 125
126 excluded. 126
127 127

128 After key points detection, we summarize information about local gradient 128
129 around each key point, as shown in Fig. 1. The histogram of gradient orientation 129
130 is computed as the resulting feature vector. In our work, we extract 4×4 his- 130
131 tograms with 8 orientation bins for each candidate region. The final dimension 131
132 of SIFT feature is $4 \times 4 \times 8 = 128$. 132

133 Histogram of Oriented Gradient (HOG) divides the image region into a cell- 133
134 block structure and generates histogram based on the gradient orientation and 134

135
136
137
138
139
140
141
142
143
144
145
146
147
148
149
150
151
152
153
154
155
156
157
158
159
160
161
162
163
164
165
166
167
168
169
170
171
172
173
174
175
176
177
178
179

135
136
137
138
139
140
141
142
143
144
145
146
147
148
149
150
151
152
153
154
155
156
157
158
159
160
161
162
163
164
165
166
167
168
169
170
171
172
173
174
175
176
177
178
179

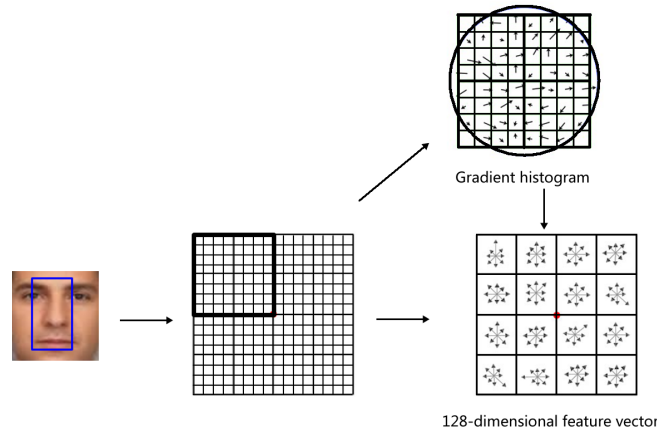


Fig. 1. SIFT feature extraction

spatial location. The input region (block) is divided into small connected regions, called cells, and for each cell a histogram of edge orientations is computed. The histogram channels are evenly spread from 0 to 180 degrees. The histogram counts are normalized for illumination compensation. This can be done by accumulating a measure of local histogram energy over the somewhat larger connected regions and using the results to normalize all cells in the block. The concatenation of these histograms yields the final HOG descriptor. In our case, we extract 4 cells and 8 gradient orientation bins for each candidate block, as shown in Fig. 2. The dimension of HOG is $4 \times 8 = 32$.

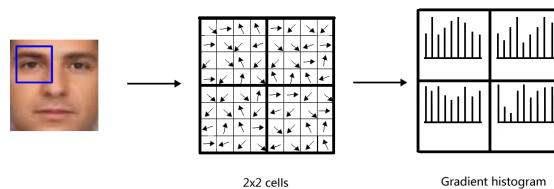


Fig. 2. HOG feature extraction

HOG is not invariant to rotation, but the computation cost is only 1/5 compared to SIFT. This will be considered in the complexity-aware process of the RealAdaBoost procedure.

3.2 Gabor filters

The Gabor wavelets, whose kernels are similar to the 2D receptive field profiles of the mammalian cortical simple cells, exhibit desirable characteristics of spatial

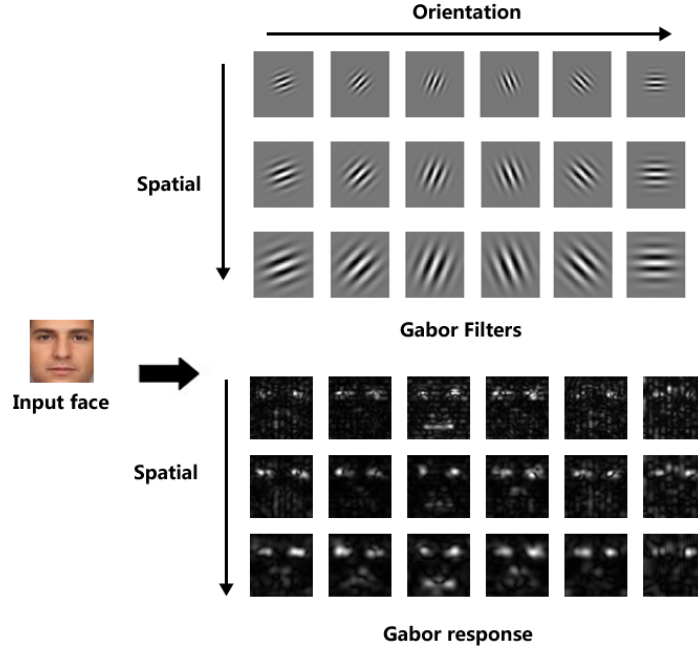


Fig. 3. Gabor filters using 3 scales and 6 orientations

locality and orientation selectivity, and are optimally localized in the space and frequency domains. The Gabor wavelets are defined in equation (1)

$$\phi_{\mathbf{k}}(\mathbf{z}) = \frac{\mathbf{k}^2}{\sigma^2} e^{\frac{\mathbf{k}^2 \mathbf{z}^2}{2\sigma^2}} [e^{i\mathbf{k}\mathbf{z}} - e^{-\frac{\sigma^2}{2}}], \quad \dots (1)$$

where σ decides the ratio of the window width and the wave length, \mathbf{z} is the normalization vector, \mathbf{k} controls the width of the Gaussian function, the wave length and direction of the shocking part, defined as follows:

$$\mathbf{k} = k_v e^{i\phi_u},$$

where $k_v = k_{max}/f_v$ and $\phi_u = \pi u/n$. k_{max} is the maximum frequency, f is the spacing factor between kernels in the frequency domain, n is the maximum orientation number.

The Gabor wavelets in (1) can be generated from the mother wavelet, by scaling and rotation via the wave vector \mathbf{k} . Each kernel is a product of a Gaussian envelope and a complex plane wave, while the first term in the square brackets in (1) determines the oscillatory part of the kernel and the second term compensates for the DC value. The effect of the DC term becomes negligible when the parameter σ , which determines the ratio of the Gaussian window width to wavelength, has sufficiently large values. In our case, we utilize three scales and six orientations to represent the components. And we set

225
226
227
228
229
230
231
232
233
234
235
236
237

$$\sigma = 2\pi \quad k_{max} = \frac{\pi}{2} \quad f = \sqrt{2}.$$

225
226
227
228
229
230
231
232
233
234
235
236
237

An example of the extracted Gabor features of an input face are illustrated in Fig. 3.

The feature dimension of dense Gabor feature depends on the size of the block, it will be quite high if we want to extract features in a large region. So we utilize a sub-sampling strategy, which applies a 2×2 to 6×6 sub-sampling based on the block size. The Gabor features are extracted only on the sub-sampled pixels. Using this strategy, the minimum feature dimension of Gabor is $3 \times 6 \times 9 = 162$ (6×6 block with 2×2 sub-sampling), and the maximum is $3 \times 6 \times 30 = 540$ (32×40 block with 6×6 sub-sampling).

4 LEARNING THE FEATURES USING REALADABOOST WITH COMPLEXITY PENALTY TERMS

238
239
240
241
242
243
244
245
246
247
248
249
250

We utilize RealAdaBoost to select the key features classifying each age group respectively. In RealAdaBoost, an image feature can be seen as a function from the image space to a real valued range $f : \mathbf{x} \rightarrow [f_{min}, f_{max}]$. The weak classifier based on f is a function from the feature vector \mathbf{x} to a real valued classification confidence space. For the binary classification problem, suppose the training data as $(\mathbf{x}_1, y_1), \dots, (\mathbf{x}_n, y_n)$ where \mathbf{x}_i is the training sample and $y \in \{-1, 1\}$ is the class label, we first divide the sample space into N_b several equal sized sub-ranges B_j

238
239
240
241
242
243
244
245
246
247
248
249
250

$$X_j = \{\mathbf{x} | f(\mathbf{x}) \in B_j\}, j = 1, \dots, N_b. \quad \dots (2)$$

The weak classifier is defined as a piecewise function

251
252
253
254
255
256

$$h(\mathbf{x}) = \frac{1}{2} \ln \left(\frac{W_+^j + \epsilon}{W_-^j + \epsilon} \right), \quad \dots (3)$$

251
252
253
254
255
256

where ϵ is the smoothing factor, W_{\pm} is the probability distribution of the feature value for positive/negative samples, implemented as a histogram

257
258
259
260

$$W_{\pm}^j = P(\mathbf{x} \in X_j, y \in \{-1, 1\}), j = 1, \dots, N_b. \quad \dots (4)$$

257
258
259
260

The best weak classifier is selected according to the classification error Z of the piecewise function in equation (5)

261
262
263
264
265

$$Z = 2 \sum_j \sqrt{W_+^j W_-^j}. \quad \dots (5)$$

261
262
263
264
265

We adopt RealAdaBoost to learn the key regions and the type of feature extraction methods. In consideration of the efficiency, we add a complexity-aware criteria into the decision term of RealAdaBoost, as shown in equation (6)

266
267
268
269

266
267
268
269

270
271
272
273
274
275
276
277
278
279
280
281
282
283
284
285
286
287
288
289
290
291
292
293
294
295
296
297
298
299
300
301
302
303
304
305
306
307
308
309
310
311
312
313
314

270
271
272
273
274
275
276
277
278
279
280
281
282
283
284
285
286
287
288
289
290
291
292
293
294
295
296
297
298
299
300
301
302
303
304
305
306
307
308
309
310
311
312
313
314

$$Z = 2 \sum_j \sqrt{W_+^j W_-^j} + a \cdot fp \cdot C, \quad \dots (6)$$

where C is the computation cost of the features, a is the complexity-aware factor to balance the discriminative capability and the computation complexity, fp is the false positive rate of current stage. In the training procedure, features with minimum Z are selected.

The equation (5) could be explained as follows, in the first stages of RealAdaBoost, the age group of faces are still easy to be classified, so efficient features are preferred. In the following stages, the patterns of the training samples are complicated. Then the features with high computation cost are considered.

We apply the above RealAdaBoost on the 4 age group classification tasks respectively. In each task, the positive samples are the samples in that age group, while the negative samples are the combination of all samples in other 3 groups. To evaluate the computation cost, we test the execution time of different feature extraction modules and set the C of SIFT to 10, HOG to 2, and Gabor to 3-6 based on its dimension. The complexity-aware factor a is set to 0.15 in our experiment. The diagram of the whole complexity-aware RealAdaBoost is illustrated in Fig. 4.

Parameters
N number of training samples
M number of evaluated features each iteration
T maximum number of weak classifiers
Input: Training set
$\{(\mathbf{x}_i, y_i)\}, i = 1, \dots, N, \mathbf{x}_i \in R^d, y_i \in \{-1, 1\}$
1. Initialize sample weight, classifier output, and false positive rate
$w_i = \frac{1}{N}, F(\mathbf{x}_i) = 0, i = 1, \dots, N, fp_0 = 1$
2. Repeat for $t = 1, 2, \dots, T$
2.1 Update the sample weight w_i using the h^{th} weak classifier output
$w_i = w_i e^{-y_i h_i(\mathbf{x}_i)}$
2.2 For $m = 1$ to M
2.2.1 Generate a random region with a specific feature extraction method (SIFT, HOG, or Gabor)
2.2.2 Extract features and do least square to $y_i \in \{-1, 1\}$
2.2.3 Build the predict distribution function W_+ and W_-
2.2.4 Select the best feature which minimizes Z in equation (6)
2.3 Update weak classifier using (3)
2.4 Update strong classifier $F_{t+1}(\mathbf{x}_i) = F_t(\mathbf{x}_i) + h_t(\mathbf{x}_i)$
2.5 Calculate current false positive rate fp_t
3. Output classifier $F(\mathbf{x}) = \text{sign}[\sum_{j=1}^T h_j(\mathbf{x})]$

Fig. 4. Learning the features using RealAdaBoost with complexity penalty term

315
316
317
318
319
320
321
322
323
324
325
326
327
328
329
330
331
332
333
334
335
336
337
338
339
340
341
342
343
344
345
346
347
348
349
350
351
352
353
354
355
356
357
358
359

5 Experiments

5.1 Experiments setup

In the experiments, two databases are used to evaluate the performance of the proposed method: the PAL aging database and the FG-NET aging database. The PAL aging database contains 430 Caucasians with age range 18-93 years old [17]. The images in the database were captured using a digital camera with fixed light and position conditions. The resolution of the images is 640×480 pixels. This database includes various expressions such as smiling, sadness, anger, or neutral faces. In the experiments, we used only neutral faces in order to exclude the facial expression effect. Sample images used in our experiments are shown in Fig. 5.



Fig. 5. Sample images in PAL aging database

The FG-NET aging database [18] is one of the most frequently used database for estimating age in the previous works. The database has 1,002 images composed of 82 Europeans in the age range 0-69 years old. Individuals in the database have one or more images included at different ages. These Images were obtained by scanning. Therefore, there are extreme variations in lighting, expression, background, pose, resolution and noise from scanning. Sample images of the FG-NET aging database are shown in Fig. 6.

With the PAL aging databases, five-folds cross validations are performed to evaluate the performance, which is similar to [19]. The age and gender are evenly distributed each fold. With the FG-NET aging database, Leave-One-Person-Out (LOPO) is performed because it contains a number of images of the same person. That means, 82-folds are used on the FG-NET aging database.

We divide the training samples into 4 age groups, 0-15, 16-40, 41-59, and 60+. The complexity-aware RealAdaBoost is applied on each group classification to select the meaningful features. Moreover, a two-steps hierarchical classifier is further adopted to generate the final age estimator. Firstly, linear support vector

315
316
317
318
319
320
321
322
323
324
325
326
327
328
329
330
331
332
333
334
335
336
337
338
339
340
341
342
343
344
345
346
347
348
349
350
351
352
353
354
355
356
357
358
359



Fig. 6. Sample images in FG-NET aging database

machine based age group classification is trained based on the selected features. Then we use the support vector regression to estimate the exact age in each age group.

The evaluation is based on the Mean Absolute Error (MAE) and the Cumulative Score (CS). The MAE is defined as the mean of the absolute difference between the estimated age and the real age, as

$$MAE = \frac{\sum_{i=1}^N |e_i - g_i|}{N},$$

where N is the number of the test images, e_i is the estimated age of the test image i and g_i is the ground-truth age. The Cumulative Score(CS) is defined as the ratio of the number of data whose errors are lower than a threshold, as

$$CS = \frac{N_{error \leq threshold}}{N}.$$

Table 1. MAE in PAL database. Units: years old

Approach	Mean Absolute Error (MAE)
SIFT	5.98
HOG	6.14
Gabor	5.88
SIFT + HOG	5.54
SIFT + Gabor	5.05
HOG + Gabor	5.57
All three features	4.29
[19]	5.36
[9]	4.33
[20]	4.52

405 **5.2 Experimental results**

406 We train 7 age estimators using the proposed framework, which includes the
 407 classifiers utilizing single feature (SIFT, HOG, and Gabor), the combination of
 408 two features, and all of the three features. There are no complexity-aware pro-
 409 cedure if single feature is adopted. Table 1 and table 2 present the MAE of
 410 these age estimators in the PAL database and FG-NET database. It can be seen
 411 that using the complexity-aware feature combination, the estimation accuracy is
 412 significantly improved compared to using SIFT, HOG, or Gabor independently.
 413 Using all three features, the MAE is further reduced. The accuracy is also com-
 414 parable with the state-of-the-art algorithms in both of the two datasets.
 415

416 **Table 2.** MAE in FG-NET database. Units: years old

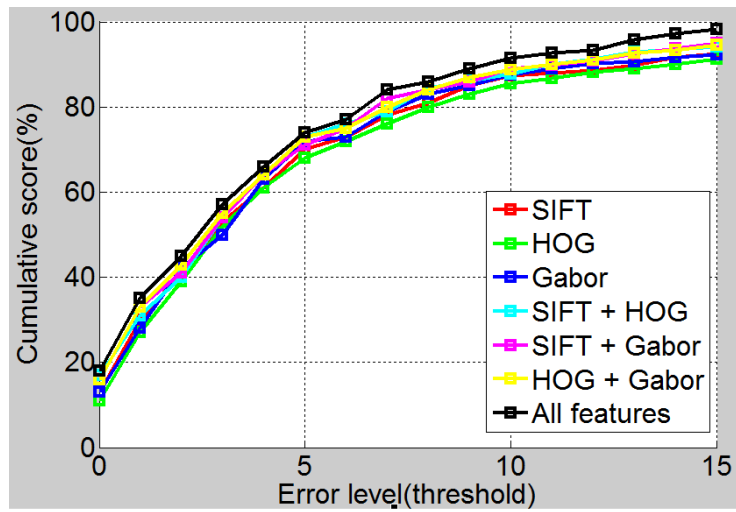
Approach	Mean Absolute Error (MAE)
SIFT	5.97
HOG	5.86
Gabor	5.68
SIFT + HOG	5.27
SIFT + Gabor	5.09
HOG + Gabor	5.10
All three features	4.49
[21]	5.05
[9]	4.66
[22]	4.67

417 We also plot the curve of the cumulative scores for the above 7 age estimators
 418 in Fig. 7. It can be seen that the cumulative score moved up at a clear border on
 419 the PAL database and FG-NET database using the proposed complexity-aware
 420 method (black curve). This result also shows the effectiveness of our method.
 421
 422
 423
 424
 425
 426
 427
 428
 429
 430
 431
 432
 433

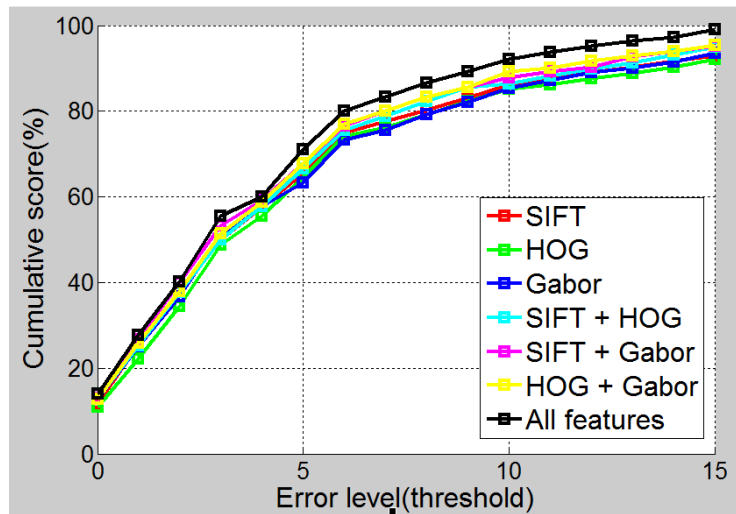
434 **5.3 Analysis**

435 We draw the first 7 features selected by the RealAdaBoost algorithm in LFW
 436 database, as shown in Fig. 8. There are 2 SIFT features, 3 HOG features, and 2
 437 Gabor features. It could be seen that most of the features lays on the eyes and
 438 mouth region. This result is reasonable, because it is much easier to estimate the
 439 age from eye and mouth rather than other face regions such as nose or eyebrow.
 440

441 We test the resulting classifiers on a desktop PC with a 2.5 GHz I3 PC and 2
 442 GB memory. The execution speed is shown in Table 3. We find that the estimator
 443 based on SIFT is relatively slow compared to the one using HOG or Gabor. If
 444 we combine these features together and use the complexity-aware strategy, the
 445
 446
 447
 448
 449



(a) CS on PAL dataset



(b) CS on FG-NET dataset

Fig. 7. CS on PAL and FG-NET database

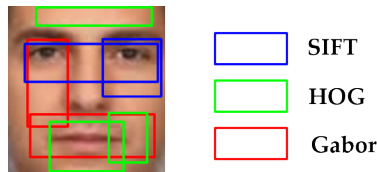


Fig. 8. The first 7 features selected by RealAdaBoost in human face

495 execution time will be reduced, shown as the rows with asterisks. Furthermore, if
496 all three features are used, the speed is significantly improved from 26.88ms per
497 face to 12.22ms per face using the complexity-aware RealAdaBoost. So we can
498 get the conclusion that the proposed method contributes to both the accuracy
499 and the efficiency of age estimation.

500

501

502 **Table 3.** Execution Speed of age estimators. Item with * denotes that the complexity-
503 aware strategy is adopted.

503

504

505

506

507

508

509

510

511

512

513

514

515

516

517

518

519

520

6 Conclusion

521

522

523

524

525

526

527

528

529

530

531

532

533

534

535

536

537

538

539

521 In this paper, we proposed a local feature-based face representation for age
522 estimation. We used a RealAdaBoost algorithm with the complexity penalty
523 term to select the meaningful features, which successfully balances the accuracy
524 and efficiency. High age estimation accuracy were reported in comparison to
525 previously published results on two famous datasets. 4.29 MAE was achieved for
526 PAL, and 4.49 was achieved for FG-Net.

527 The approach proposed in this paper could be further studied. We have
528 already found that the proposed framework is also effective on other recognition
529 tasks, such as gender recognition and emotion recognition.

530

531

532

533

534

535

536

537

538

539

References

1. Milborrow, S., Nicolls, F.: Locating facial features with an extended active shape model. In: Computer Vision–ECCV 2008. Springer (2008) 504–513
2. Cootes, T.F., Edwards, G.J., Taylor, C.J., et al.: Active appearance models. IEEE Transactions on pattern analysis and machine intelligence **23** (2001) 681–685
3. Shan, C.: Learning local features for age estimation on real-life faces. In: Proceedings of the 1st ACM international workshop on Multimodal pervasive video analysis, ACM (2010) 23–28

- 540 4. Kwon, Y.H., da Vitoria Lobo, N.: Age classification from facial images. In: Com- 540
541 puter Vision and Pattern Recognition, 1994. Proceedings CVPR'94., 1994 IEEE 541
542 Computer Society Conference on, IEEE (1994) 762–767 542
543 5. Hayashi, J., Yasumoto, M., Ito, H., Koshimizu, H.: Method for estimating and 543
544 modeling age and gender using facial image processing. In: Virtual Systems and 544
545 Multimedia, 2001. Proceedings. Seventh International Conference on, IEEE (2001) 545
546 439–448 546
547 6. Fukai, H., Takimoto, H., Mitsukura, Y., Fukumi, M.: Apparent age estimation 547
548 system based on age perception. Proc. of SICE (2007) 2808–2812 547
549 7. Gao, F., Ai, H.: Face age classification on consumer images with gabor feature and 548
549 fuzzy lda method. In: Advances in biometrics. Springer (2009) 132–141 549
550 8. Mu, G., Guo, G., Fu, Y., Huang, T.S.: Human age estimation using bio-inspired 550
551 features. In: Computer Vision and Pattern Recognition, 2009. CVPR 2009. IEEE 551
552 Conference on, IEEE (2009) 112–119 552
553 9. Choi, S.E., Lee, Y.J., Lee, S.J., Park, K.R., Kim, J.: Age estimation using a 553
554 hierarchical classifier based on global and local facial features. Pattern Recognition 554
555 **44** (2011) 1262–1281 555
556 10. Lanitis, A., Taylor, C.J., Cootes, T.F.: Toward automatic simulation of aging ef- 556
557 fects on face images. Pattern Analysis and Machine Intelligence, IEEE Transactions 557
558 on **24** (2002) 442–455 558
559 11. Ueki, K., Hayashida, T., Kobayashi, T.: Subspace-based age-group classification 559
560 using facial images under various lighting conditions. In: Automatic Face and 560
561 Gesture Recognition, 2006. FGR 2006. 7th International Conference on, IEEE 561
562 (2006) 6–pp 562
563 12. Wang, J.G., Sung, E., Yau, W.Y.: Active learning with the furthest nearest neigh- 563
564 bor criterion for facial age estimation. In: Computer Vision–ACCV 2010. Springer 564
565 (2011) 11–24 565
566 13. Guo, G., Wang, X.: A study on human age estimation under facial expression 566
567 changes. In: Computer Vision and Pattern Recognition (CVPR), 2012 IEEE Con- 567
568 ference on, IEEE (2012) 2547–2553 568
569 14. Liu, J., Ma, Y., Duan, L., Wang, F., Liu, Y.: Hybrid constraint svr for facial age 569
570 estimation. Signal Processing **94** (2014) 576–582 570
571 15. Luu, K., Ricanek, K., Bui, T.D., Suen, C.Y.: Age estimation using active ap- 571
572 pearance models and support vector machine regression. In: Biometrics: Theory, 572
573 Applications, and Systems, 2009. BTAS'09. IEEE 3rd International Conference on, 573
574 IEEE (2009) 1–5 574
575 16. Kohli, S., Prakash, S., Gupta, P.: Hierarchical age estimation with dissimilarity- 575
576 based classification. Neurocomputing **120** (2013) 164–176 576
577 17. Minear, M., Park, D.C.: A lifespan database of adult facial stimuli. Behavior 577
578 Research Methods, Instruments, & Computers **36** (2004) 630–633 578
579 18. <http://www.fgnet.rsunit.com/>: (The fg-net aging database) 579
580 19. Suo, J., Wu, T., Zhu, S., Shan, S., Chen, X., Gao, W.: Design sparse features 580
581 for age estimation using hierarchical face model. In: Automatic Face & Gesture 581
582 Recognition, 2008. FG'08. 8th IEEE International Conference on, IEEE (2008) 1–6 582
583 20. Guo, G., Mu, G., Fu, Y., Dyer, C., Huang, T.: A study on automatic age estima- 583
584 tion using a large database. In: Computer Vision, 2009 IEEE 12th International 584
585 Conference on, IEEE (2009) 1986–1991

14 ACCV-14 submission ID 20

585	22. Chen, K., Gong, S., Xiang, T., Loy, C.C.: Cumulative attribute space for age and	585
586	crowd density estimation. In: Computer Vision and Pattern Recognition (CVPR),	586
587	2013 IEEE Conference on, IEEE (2013) 2467–2474	587
588		588
589		589
590		590
591		591
592		592
593		593
594		594
595		595
596		596
597		597
598		598
599		599
600		600
601		601
602		602
603		603
604		604
605		605
606		606
607		607
608		608
609		609
610		610
611		611
612		612
613		613
614		614
615		615
616		616
617		617
618		618
619		619
620		620
621		621
622		622
623		623
624		624
625		625
626		626
627		627
628		628
629		629